

Supporting information

Experimental procedures

Pd catalyst loading on carbon support: 0.040 g Ketjen carbon (C) was suspended in 30 mL of hexane for 1 h through sonication. Then 0.010 g of as-synthesized Pd NPs in 5 mL of hexane dispersion were added dropwise to the sonicated C-hexane suspension, which was allowed to sonicate for 1 h. The Pd/C product was then washed twice with ethanol (separated by centrifugation at 9000 rpm for 8 minutes) and dried in air. The dried Pd/C powder was suspended in 40 mL of acetic acid in a reaction flask under a nitrogen blanket and was heated to 70 °C overnight. After that, the activated Pd/C catalyst was washed once with pure ethanol and then twice more with 1:9 hexane:ethanol (separated by centrifugation at 9000 rpm for 8 min) before being dried again in air.

Pure CO₂ capture by KOH-ethylene glycol solution: Potassium hydroxide (KOH, 2.5 mmol) was dissolved into 5 mL of ethylene glycol (EG) by magnetic stirring. CO₂ was then bubbled through the solution at a rate of 0.4 L/min for 40 min at 1 psi.² The amount of captured CO₂ was estimated by comparing the total weight of the solution before and after CO₂ absorption.

Alkyl carbonate hydrogenation reaction: The captured CO₂ was hydrogenated in the capture solution without separation. Once KOH was fully utilized, the capture solution was purged with N₂ to remove the dissolved free CO₂ from the solution. 10 mg of Pd/C catalysts and 100 mg of ammonia borane were added into the reaction solution. The solution was then sealed with a balloon. The reaction mixture was stirred and heated at 50 °C (or another temperature). Once the reaction was over, a small amount of aliquot was taken for ¹H and ¹³C nuclear magnetic resonance (NMR) measurements to characterize the liquid product, and the gas product was analyzed by gas chromatography (GC).

Carbonate/bicarbonate hydrogenation reaction: 2.5 mmol of potassium carbonate/bicarbonate, 10 mg of Pd/C catalysts and 100 mg of ammonia borane were dissolved in 5 mL of EG. The reaction system was sealed with a balloon, and heated at 50 °C for 6 hours. Once the reaction was over, the solution product and gas products were analyzed by NMR and GC, respectively.

Au nanowire (NW) synthesis and electrode preparation: The synthetic method was modified from our previous publication.³ 80 mg HAuCl₄ was dissolved in 20 ml of hexane and 1.5 ml of oleylamine at room temperature under magnetic stirring. 4 ml of triisopropylsilane was then added to this solution. One minute later, magnetic stirring was stopped, and the solution was kept still at room temperature for 24 h before ethanol was added to collect NW product via centrifugation (6000 rpm, 1 min). The product was redispersed in 20 ml hexane, precipitated out again by adding 40 ml of ethanol, centrifuged (6000 rpm, 1 min), and re-dispersed in hexane.

10 mg Au NWs were deposited onto 30 mg Ketjen Carbon (C) (EC300J) by mechanically string the mixture of Au NW and carbon suspension in 60 mL hexane for 30 min. The carbon loaded catalyst was separated from hexane by centrifugation under 9000 rpm for 1 min. To remove excess ligands, the catalyst was further washed by hexane twice and dried under vacuum.

10 mg of the dried catalyst powder was ground with 2 mg polyvinylidene fluoride (PVDF) (industrial adhesive) with a few drops of 1-methyl-2-pyrrolidone (NMP) (solvent) to produce catalyst paste that was painted directly onto a 1.0 cm x 1.0 cm carbon paper (Toray TGP-H060).

The catalyst-decorated carbon paper was dried in a vacuum-oven overnight and served as a working electrode.

Alkyl carbonate electrolysis after direct air capture: An EC-Lab VSP Ultimate electrochemical workstation was used to conduct alkyl carbonate electroreduction in a three-electrode system. The experiment was performed in a gas-tight cell with two-compartments separated by a cation exchange membrane (Nafion® 117). Each compartment contained 10 mL electrolyte with approximately 10 mL headspace. All electrochemical data were collected under N₂ condition to remove dissolved CO₂ and O₂ in the electrolyte. The catholyte is 2 M potassium alkyl carbonate in EG obtained after direct air capture as shown previously. The anolyte was always 1 M KOH solution. The as-prepared Au NW/C electrode was used as the working electrode. A platinum mesh was used as the counter electrode. All potentials were measured against an Ag/AgCl reference electrode (4.0 M KCl, Pine instrument). The potentials were not IR-corrected.

Characterization

Transmission electron microscopy (TEM) images were acquired from a Philips CM20 (200 kV). Samples for TEM analyses were prepared by depositing a single drop of diluted NP dispersion/suspension on amorphous carbon-coated copper grids. X-ray diffraction (XRD) patterns were collected on a Bruker AXS D8-Advance diffractometer with Cu K α radiation ($\lambda = 1.5406 \text{ \AA}$). Inductively coupled plasma-atomic emission spectroscopy (ICP-AES) was carried out on a JY2000 Ultrace ICP-AES equipped with a JY-AS 421 autosampler and 2400 g mm⁻¹ holographic grating. The NMR characterization was carried out on a Bruker DRX (¹H, 400 MHz; ¹³C, 101 MHz). The ¹H and ¹³C NMR shifts are referenced relative to the solvent signal (d₆-DMSO; ¹H, 2.50 ppm; ¹³C, 39.52 ppm). DMF was used as an internal standard for product quantification. For quantitative ¹³C NMR, relaxation delay time was set to be 60 s. The gas product composition was analyzed by GC. The GC analysis was set up to split the gas sample into two aliquots whereof one aliquot was routed through a packed Mole Sieve 5A column and a packed HP-PLOT Q column before passing a thermal conductivity detector (TCD) for CO quantification. Argon (Corp Brother, 99.9999%) and Helium (Corp Brother, 99.9999%) were employed as carrier or make-up gasses, respectively. The second aliquot was routed through a packed HP-PLOT Q + PT column equipped with a flame ionization detector (FID) for analyzing C₁ to C₃ hydrocarbons. The GC was calibrated using commercially available calibration standards from JJS Technical Services.

Computational Methods

Electronic structure calculations were performed using the Grid-based Projector-Augmented Wave (GPAW) calculator⁴ in the Atomic Simulation Environment (ASE)⁵. A face-centered cubic (fcc) (211) unit cell of Palladium (Pd) was constructed with a size of $3 \times 4 \times 3$ atoms and 15 \AA of vacuum was spaced between slabs with the calculated lattice constant of 4.01 \AA . GPAW was employed with a finite-difference basis set with a grid spacing of 0.2 and a $4 \times 3 \times 1$ k -point mesh. The Bayesian error estimation functional with van der Waals correlation (BEEF-vdW) was used for exchange-correlation functional. Dipole-correction was performed in the xy -plane. A Fermi-level smearing width of 0.1 eV was used to help convergence, and potential energies were extrapolated back to 0 K. For finding a transition path for each step, the Dynamic nudged elastic band (DyNEB) method was utilized with the maximum force (f_{max}) of 0.03 eV/ \AA .⁶ For dissolved species in the liquid phase, we calculated their chemical potential by assuming a realistic vapor pressure, and calculating the free energy of the vapor in this low-pressure limit: we assumed that

the vapor pressure of the EG and carbon dioxide (CO₂) complex (EG-CO₂) is equal to that of the EG. And for the estimate of EG vapor pressure, we used the following equation [Eq 1].

$$\log_e P[kPa] = -25.9971 \log_e T[K] - \frac{14768.57}{T[K]} + 191.4250 + 2.062331 \times 10^{-5} \times T[K]^2 \quad [\text{Eq1}]$$

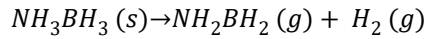
A gas-phase correction⁷ of -0.56 eV and -0.34 eV was made to CO₂ and HCOOH, respectively, as suggested by Granda-Marulanda et al.⁸ Since the EG-CO₂ complex is created by purging 413 ppm of air into KOH dissolved EG solution, a pH correction for state 1 was performed to correct the energy derived from the participation of protons in the reaction by following equations [Eq 2-3].⁹ pH of EG+KOH+CO₂ was 7.8 after CO₂ saturation.

$$G(pH) = -kT * \ln 10 \quad [\text{Eq2}]$$

$$\Delta G = G_{step2} - (G_{step1} + kT * \ln 10 * pH(7.8)) \quad [\text{Eq3}]$$

$$G_{step2} - (G_{step1} + 0.5eV)$$

To estimate the free energy for hydrogen production from ammonia borane (NH₃BH₃), we referred to previous papers,¹⁰⁻¹¹ and used the following equation:



Based on the enthalpy and entropy values of each component in different phases, we can calculate the free energy. The data used in this study are listed below:

	$\Delta H_f^o(298K) (kcal/mol)$	$S^o(298K) (cal/mol \cdot K)$
NH ₃ BH ₃ (s)	-36.5	23.0
NH ₂ BH ₂ (g)	-18.6	56.0
H ₂ (g)	0.08	31.1

The partial pressure of NH₂BH₂ was assumed to be equivalent to that of EG due to their complete dissolution in EG. As the enthalpy and entropy values are not significantly affected by temperature, the values at 298K were utilized. The entropy value, initially set at 1 atm at 298K, was adjusted to account for the partial pressure. This assumption was based on the assumption that NH₂BH₂ behaves similarly to EG. The entropy values were significantly small, resulting in similar values for both 1 atm and the partial pressure. Consequently, we only needed to adjust the temperature term in the equation $G = H - TS$ from 298K to 323.15K to calculate the final free energy for hydrogen production from NH₃BH₃.

Figures and tables

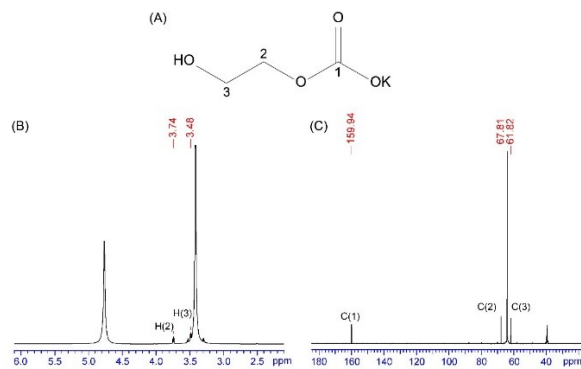


Figure S1. (A) Chemical structure of alkyl carbonate. (B) ^1H and (C) ^{13}C NMR spectra of EG solution after CO_2 capture. The ^1H and ^{13}C NMR shifts are referenced relative to the solvent signal (d_6 -DMSO; ^1H , 2.50 ppm; ^{13}C , 39.52 ppm).

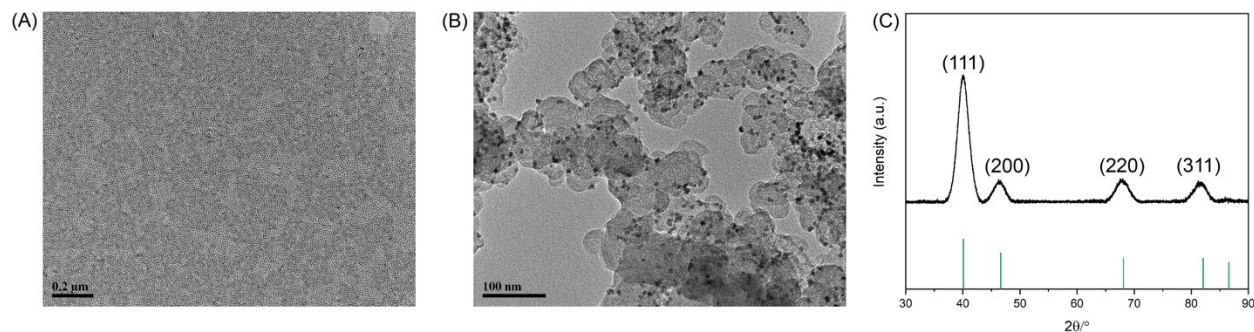


Figure S2. (A) Transmission electron microscopy (TEM) image of the as-synthesized 5 nm Pd NPs. (B) TEM image of the activated Pd/C catalyst after acetic acid wash. (C) XRD patterns of Pd NPs, JCPDS card number 00-001-1201.

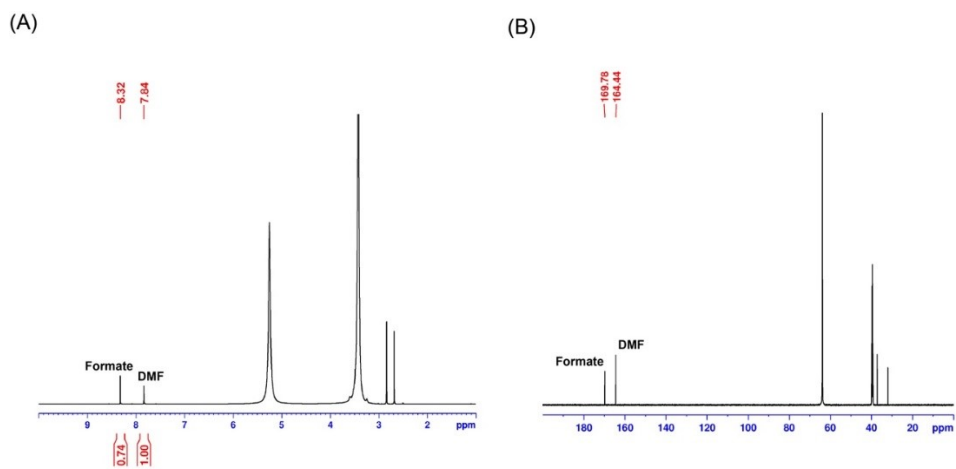


Figure S3. (A) ^1H and (B) ^{13}C NMR spectra of CO_2 loaded solution after hydrogenation reaction in d_6 -DMSO. The ^1H and ^{13}C NMR shifts are referenced relative to the solvent signal (d_6 -DMSO; ^1H , 2.50 ppm; ^{13}C , 39.52 ppm).

Table S1. Control experiments on catalyst usage.

Entry	T (°C)	Time (h)	Cat. (mol%)	Formate (%)
1	50	6	0.1	92
2	50	6	0.2	90
3	50	6	0	11
4	50	48	0	12

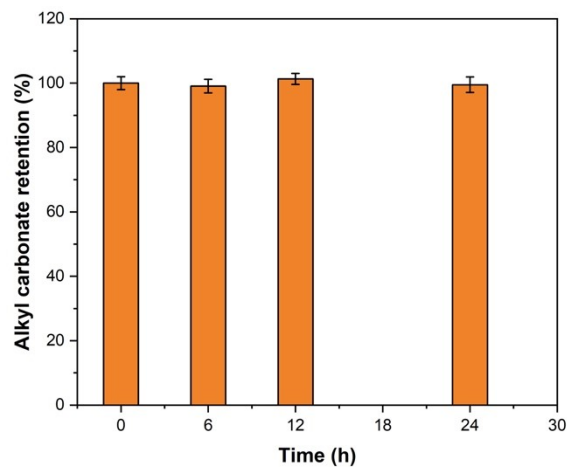


Figure S4. Alkyl carbonate retention ratio in the solution after heating for multiple hours at 120 °C.

Table S2. Control experiments on the hydrogen source.

Entry	T (°C)	Time (h)	Hydrogen source	Formate (%)
1	50	6	NH ₃ BH ₃	92
2	50	6	NaBH ₄	90
3	50	6	H ₂	7

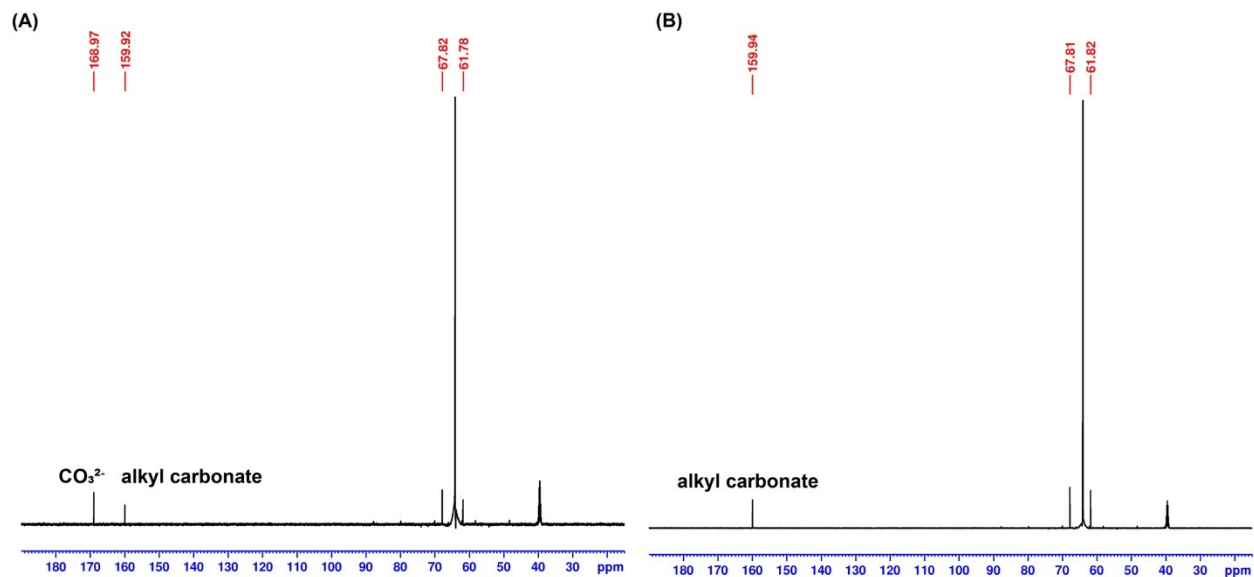


Figure S5. ^{13}C NMR spectra of (A) carbonate salt (K_2CO_3) dissolved in ethylene glycol and (B) bicarbonate salt (KHCO_3) dissolved in ethylene glycol. The ^{13}C NMR shifts are referenced relative to the solvent signal (d_6 -DMSO; ^{13}C , 39.52 ppm).

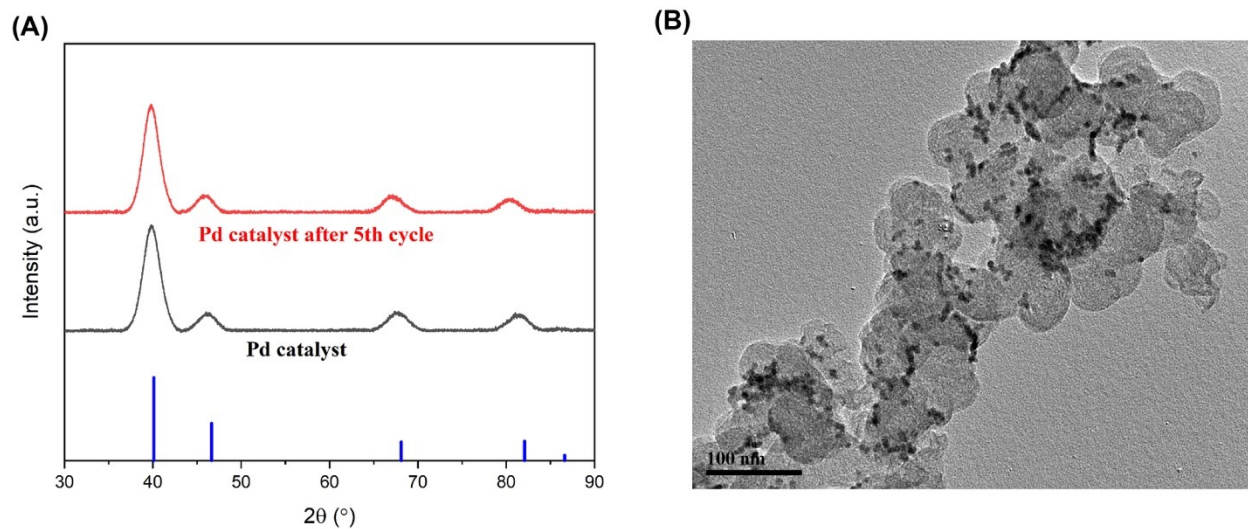


Figure S6. (A) XRD patterns and (B) TEM image of Pd catalysts after 5th catalytic cycles.

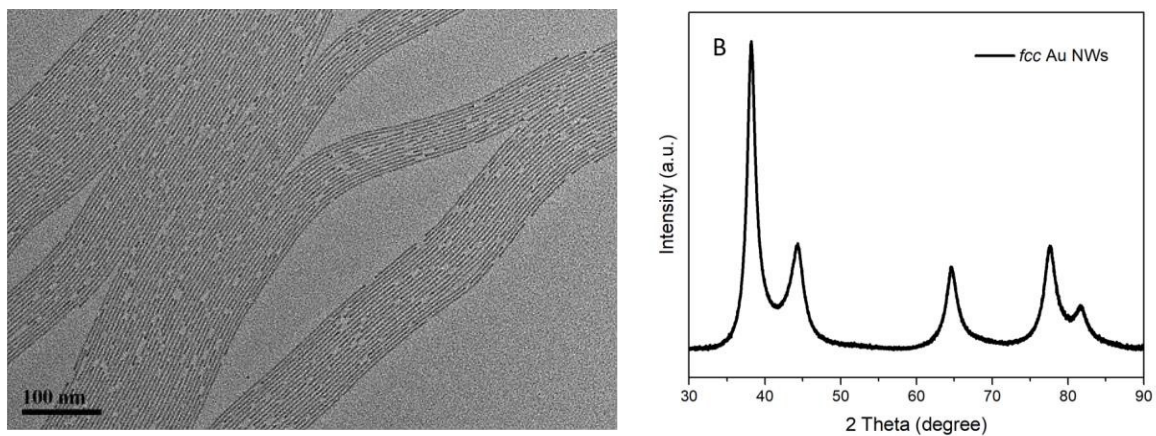


Figure S7. A) TEM of Au nanowires. B) XRD pattern of Au nanowires.

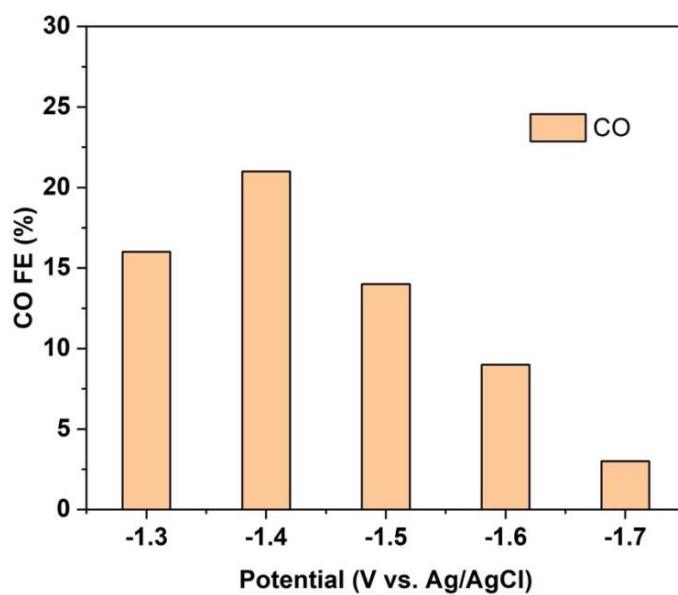


Figure S8. Potential-dependent CO FE obtained from Au NW-catalyzed electroreduction of alkyl carbonate in the capture solution.

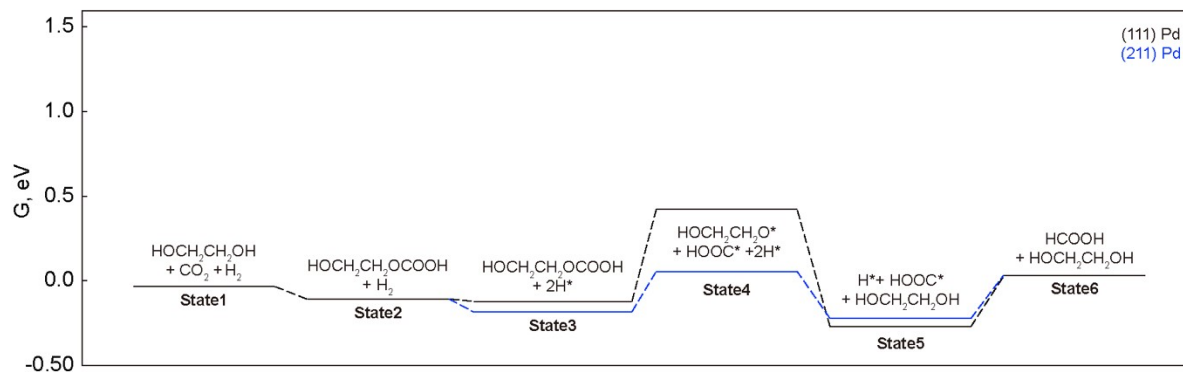


Figure S9. Comparison of free energy diagrams for the (111) and (211) facets of Pd. Black bars represent (111) Pd, and blue bars represent (211) Pd. Note: The parameters used in all calculations are the same as those used in the main calculation (**Figure 5**), but only the lattice constant was calculated with the experimental value, 3.98 Å.

Reference

1. Mazumder, V.; Sun, S., Oleylamine-Mediated Synthesis of Pd Nanoparticles for Catalytic Formic Acid Oxidation. *J. Am. Chem. Soc.* **2009**, *131* (13), 4588-4589.
2. Sen, R.; Goepfert, A.; Kar, S.; Prakash, G. K. S., Hydroxide Based Integrated CO₂ Capture from Air and Conversion to Methanol. *J. Am. Chem. Soc.* **2020**, *142* (10), 4544-4549.
3. Zhu, W.; Zhang, Y.-J.; Zhang, H.; Lv, H.; Li, Q.; Michalsky, R.; Peterson, A. A.; Sun, S., Active and Selective Conversion of CO₂ to CO on Ultrathin Au Nanowires. *J. Am. Chem. Soc.* **2014**, *136* (46), 16132-16135.
4. Mortensen, J. J.; Hansen, L. B.; Jacobsen, K. W., Real-space grid implementation of the projector augmented wave method. *Phys. Rev. B* **2005**, *71* (3), 035109.
5. Hjorth Larsen, A.; Jørgen Mortensen, J.; Blomqvist, J.; Castelli, I. E.; Christensen, R.; Dułak, M.; Friis, J.; Groves, M. N.; Hammer, B.; Hargus, C.; Hermes, E. D.; Jennings, P. C.; Bjerre Jensen, P.; Kermode, J.; Kitchin, J. R.; Leonhard Kolsbjerg, E.; Kubal, J.; Kaasbjerg, K.; Lysgaard, S.; Bergmann Maronsson, J.; Maxson, T.; Olsen, T.; Pastewka, L.; Peterson, A.; Rostgaard, C.; Schiøtz, J.; Schütt, O.; Strange, M.; Thygesen, K. S.; Vegge, T.; Vilhelmsen, L.; Walter, M.; Zeng, Z.; Jacobsen, K. W., The atomic simulation environment—a Python library for working with atoms. *J. Phys.: Condens. Matter* **2017**, *29* (27), 273002.
6. Lindgren, P.; Kastlunger, G.; Peterson, A. A., Scaled and Dynamic Optimizations of Nudged Elastic Bands. *J. Chem. Theory Comput.* **2019**, *15* (11), 5787-5793.
7. Peterson, A. A.; Abild-Pedersen, F.; Studt, F.; Rossmeisl, J.; Nørskov, J. K., How copper catalyzes the electroreduction of carbon dioxide into hydrocarbon fuels. *Energy Environ. Sci.* **2010**, *3* (9), 1311-1315.
8. Granda-Marulanda, L. P.; Rendón-Calle, A.; Builes, S.; Illas, F.; Koper, M. T. M.; Calle-Vallejo, F., A Semiempirical Method to Detect and Correct DFT-Based Gas-Phase Errors and Its Application in Electrocatalysis. *ACS Catal.* **2020**, *10* (12), 6900-6907.
9. Nørskov, J. K.; Rossmeisl, J.; Logadottir, A.; Lindqvist, L.; Kitchin, J. R.; Bligaard, T.; Jónsson, H., Origin of the Overpotential for Oxygen Reduction at a Fuel-Cell Cathode. *J. Phys. Chem. B* **2004**, *108* (46), 17886-17892.

10. Dixon, D. A.; Gutowski, M., Thermodynamic Properties of Molecular Borane Amines and the $[\text{BH}_4^-][\text{NH}_4^+]$ Salt for Chemical Hydrogen Storage Systems from ab Initio Electronic Structure Theory. *J. Phys. Chem. A* **2005**, *109* (23), 5129-5135.
11. Matus, M. H.; Anderson, K. D.; Camaioni, D. M.; Autrey, S. T.; Dixon, D. A., Reliable Predictions of the Thermochemistry of Boron–Nitrogen Hydrogen Storage Compounds: $\text{B}_x\text{N}_x\text{H}_y$, $x = 2, 3$. *J. Phys. Chem. A* **2007**, *111* (20), 4411-4421.